

Nuclear reactions in Rb, Sr, Y, and Zr targets

S. Regnier, B. Lavielle, M. Simonoff, and G. N. Simonoff

*Centre d'Etudes Nucléaires de Bordeaux-Gradignan, Laboratoire de Chimie Nucléaire,
Le Haut Vigneau 33170 Gradignan, France*

(Received 12 March 1982)

Excitation functions of all stable or long-lived krypton isotopes were measured or estimated for incident protons and neutrons in Rb, Sr, Y, and Zr targets. Experimental data concern mostly Y and Zr targets bombarded with 0.059 to 24 GeV protons. The products $^{78-86}\text{Kr}$, ^{74}As , ^{75}Se , $^{83,84,86}\text{Rb}$, ^{85}Sr , ^{88}Y , $^{88,95}\text{Zr}$, and $^{92}\text{Nb}^m$ were measured using high-sensitivity mass spectrometry and nondestructive γ counting. Lighter products such as $^{38,39,42}\text{Ar}$ and 12 radioactive isotopes from ^7Be to ^{65}Zn were also measured in some cases and their cross sections are given in an appendix. Most excitation functions pass through a maximum between 0.4 and 0.8 GeV, and the peak energy could depend on the ΔA value. The results, combined with a general survey of nuclear reactions in Ga to Nb targets, permitted the development of new systematics leading to the calculation of spallation-produced Kr isotopes in the moon bombarded with galactic and solar cosmic rays. Compared to cosmogenic krypton measured in nine well-documented lunar samples, ^{83}Kr is predicted with a precision better than 33% (1σ) and the production ratios $^{86}\text{Kr}/^{83}\text{Kr}$ are predicted to better than 25%. It is concluded that the cosmogenic ratios $^{86}\text{Kr}/^{83}\text{Kr}$ and $^{81}\text{Kr}/^{83}\text{Kr}$ are dependent on the main target element concentrations. This should be taken into account in strontium-rich samples when calculating exposure ages of extraterrestrial materials.

NUCLEAR REACTIONS ^{89}Y and Zr, (p , spallation) $E=0.059-24$
GeV; measured $\sigma(E)$ for $^{78-86}\text{Kr}$ and 12 radioactive products. Sys-
tematics of p - and n -induced reactions in Rb, Sr, Y, and Zr. Cosmogen-
ic krypton.

I. INTRODUCTION

Like other noble gases, krypton has been largely outgassed from most solar system materials through several heating processes. Consequently, its cosmogenic component, produced by cosmic-ray-induced nuclear reactions near the surface of atmosphere-free planetary objects, is detectable and provides a good sensor of the exposure histories of meteorites and lunar samples.^{1,2} The possibility of predicting the cosmogenic component of krypton has already been tested,^{3,4} using mainly two sets of parameters: the fluxes of galactic and solar cosmic rays as a function of depth, calculated according to the Reedy-Arnold model⁵; and cross sections of relevant nuclear reactions, the measurement of which is one purpose of the present study. The main targets for producing krypton by nuclear reactions in extraterrestrial matter are Zr, Y, Sr, and Rb, except in iron-rich objects. Rubidium has a low relative abundance in chondrites and most lunar samples,

but is able to produce ^{86}Kr and ^{84}Kr through high cross-section peripheral reactions.⁷ The galactic cosmic-rays primary flux consists mostly of several GeV protons, but its development in a thick object produces a continuous spectrum of secondary protons and neutrons until thermalization. Solar cosmic rays consist of less than 100-MeV particles and interact only in the external few centimeters of a solid object. Very different nuclear reactions are involved in the production of krypton in Zr, Y, Sr, and Rb, implying the emission of between one and 20 particles by the struck nucleus. In some cases, secondary protons and neutrons are expected to be the most efficient particles. Finally, many cross-section measurements are necessary to give a good evaluation of excitation functions. Our choice was to irradiate Y and Zr targets with 0.059 to 24 GeV protons (nine energies). We measured cross sections of krypton isotopes with $A=78, 80, 81, 82, 83, 84, 85,$ and 86 . In order to improve knowledge of nuclear reactions in the target and product mass range

of interest, we also used nondestructive γ counting for measuring ^{74}As , ^{75}Se , $^{83,84,86}\text{Rb}$, ^{85}Sr , ^{88}Y , $^{88,95}\text{Zr}$, and $^{92}\text{Nb}^m$ production cross sections. Of particular interest were the $^{89}\text{Y}(p,3p3n)^{84}\text{Rb}$, $^{89}\text{Y}(p,3pn)^{86}\text{Rb}$, $^{89}\text{Y}(p,pn)^{88}\text{Y}$, and $^{89}\text{Y}(p,2n)^{88}\text{Zr}$ reaction channels for evaluating unknown cross sections in Rb and Sr targets. This evaluation was also made possible by a general survey of nuclear reactions in Ga ($Z=31$) to Nb ($Z=41$) targets leading to newly developed systematics. By measuring $^{83,84}\text{Rb}$ production cross sections, we were able to obtain total isobaric yields for the corresponding krypton isotopes. The nine proton energies used for this study enable us to confirm observations already made in this laboratory⁶ concerning the maximum of excitation functions for spallation reactions in the GeV energy region. In most cases we also measured cross sections of argon isotopes 36, 38, 39, and 42. These results will be given in the Appendix, together with cross sections for ^7Be , ^{22}Na , ^{46}Sc , ^{48}V , ^{51}Cr , $^{52,54}\text{Mn}$, ^{59}Fe , $^{56,58,60}\text{Co}$, and ^{65}Zn , produced in Y and Zr bombarded with 1.005, 2.5, and 24 GeV protons. Implications of our new data for some cosmochemical problems will be discussed.

II. EXPERIMENTAL

Pure (99.9% or 3N) target foils of Y, Zr, and in some cases vapor deposited Sr were stacked with monitor and guard aluminum (5N) foils, each being about 20 μm thick. Exact thickness was determined by weighing. The targets were irradiated in accelerators giving several proton energies: Louvain-la-Neuve (59, 75, and 80 MeV); Orsay-SC (150, 168, and 200 MeV); Saturne II (1 and 2.5 GeV), and CERN-PS (24 GeV). Extracted beams were used in all cases, so that misalignment was not a major source of error. Special care was taken to minimize secondary particle effects. Proton fluence was measured according to the $^{27}\text{Al}(p,3p3n)^{22}\text{Na}$ monitor reaction whose cross sections are given in Table I.⁸ Between 2×10^{15} and 7×10^{16} protons struck the targets. Most irradiated Y and Zr foils were counted several times in a 4 keV resolution Ge(Li) gamma ray spectrometer, calibrated with ^{56}Co , ^{152}Eu , and ^{22}Na standards. Detected isotopes, their half-lives, γ -ray energies, and branching ratios are listed in Table II.

Several months after irradiation Y or Zr targets and blank foils were stored (ten at a time) in an extraction system in which an ultrahigh vacuum (better than 10^{-9} Torr) was progressively attained by pumping and baking all elements. Targets were

TABLE I. Cross sections for the monitor reaction $^{27}\text{Al}(p,3p3n)^{22}\text{Na}$ versus proton energy, according to Ref. 8.

E_p (GeV)	σ (mb)
0.059	28.0
0.075	23.7
0.080	22.7
0.150	17.2
0.168	16.6
0.200	16.1
1.0	15.3
1.05	15.3
2.5	11.3
24.0	10.1

baked several days at 80 to 100°C and we checked that this procedure did not outgas any spallogenic krypton. Each foil was then melted inside a molybdenum crucible heated by an electronic bombardment oven routinely operating at 1900°C. Extracted gases were exposed in two steps to Ti and CuO-Pd getters between 700° and 200°C for eliminating active species. Kr (95–98%) was then adsorbed on a first activated charcoal trap at -120° . The remainder was adsorbed together with 98–99% Ar on a second trap at -196°C . Argon and krypton were successively introduced into a statically-operated, 60° sector, 12 cm radius, MM 1202 mass spectrometer, equipped with an electron multiplier and a microcomputer-assisted peak switching and data storage unit.⁹ The mass spectrometer was calibrated by introducing air standards from a pipette or from an independent system composed of several known volumes and a capacitance manometer. During the course of these experiments, the MM 1202 was tuned for optimum

TABLE II. Some nuclear properties of the radionuclides measured in this study, taken from Ref. 11. E_γ is the gamma-ray energy and I_γ is the branching intensity.

Nuclide	E_γ (MeV)	I_γ (%)	Half-life (d)
^{74}As	0.596	60	17.79
^{75}Se	0.265	58	118.45
^{83}Rb	0.520	46	86.2
^{84}Rb	0.882	74	32.77
^{86}Rb	1.077	8.79	18.82
^{85}Sr	0.514	100	64.85
^{88}Y	0.898	94.3	106.61
	1.836	99.34	
^{88}Zr	0.394	97.3	83.4
^{95}Zr	0.757	54.6	63.98
$^{92}\text{Nb}^m$	0.934	99.2	10.14

TABLE III. Cross sections (in mb) for some radioactive isotopes produced in ^{89}Y as a function of the proton incident energy E_p (in GeV). "I" means independent cross sections. Others are cumulative.

E_p (GeV)	0.059	0.075	0.168	0.200	1.0	2.5	24.0
$^{74}\text{As}_I$					9.5 ± 1.9	5.6 ± 1.1	
^{75}Se			3.8 ± 0.8	8.5 ± 1.7	46 ± 9	21.3 ± 4.2	16.1 ± 3.2
^{83}Rb		29 ± 6	54 ± 11	55 ± 11	45 ± 9	23 ± 5	19.2 ± 3.8
$^{84}\text{Rb}_I$		5.4 ± 1.1	13.3 ± 2.6	14.4 ± 2.8	14.8 ± 3	12.0 ± 2.4	11.8 ± 2.3
$^{86}\text{Rb}_I$					6.9 ± 1.6	4.8 ± 1.1	
^{85}Sr		17 ± 7	39 ± 8	46 ± 9	50 ± 22	34.5 ± 9.3	18.2 ± 3.6
$^{88}\text{Y}_I$	195 ± 42	165 ± 37	110 ± 24	115 ± 25		63 ± 13	61 ± 12
$^{88}\text{Zr}_I$	126 ± 25	55 ± 11	18.3 ± 3.7	19.2 ± 3.8		5.9 ± 1.5	4.2 ± 0.8

stability and acted as quite a good manometer for krypton: The sensitivity for ^{82}Kr remained constant at 3.2×10^{-19} A/atom, within 5% (1σ). Flat-top peaks were obtained for a resolution of 250 (1% valley). The isotope ratios were subjected to corrections occasioned by memory or pumping effects, isotopic discrimination, blank, hydrocarbon, and doubly-charged ions. Target blanks for ^{86}Kr were 6×10^{-12} and 2×10^{-13} cm³ STP, respectively, in Y and Zr foils. Correction for hydrocarbon ions was necessary at $m/e=78$ only, and was monitored by the signal at $m/e=77$. The main problem was memory, which was lowered by frequently baking the resolving section at about 120°C.

III. RESULTS

Cross sections for radioactive isotopes ^{74}As , ^{75}Se , $^{83,84,86}\text{Rb}$, ^{85}Sr , ^{88}Y , $^{88,95}\text{Zr}$, and $^{92}\text{Nb}^m$ are presented in Sec. III A, and those for mostly-stable krypton isotopes with $A=78, 80, 81, 82, 83, 84, 85$, and 86 are dealt with in Sec. III B.

A. Radioactive isotopes

Cross sections at nine proton energies are given in Table III for Y targets (eight products) and in Table IV for Zr targets (ten products). The uncertainties shown were calculated as follows. Homogeneity and purity of target foils introduced a less than 1% error. Errors associated with monitoring were 2–4% for counting of ^{22}Na and 10% for the $^{27}\text{Al}(p,3p3n)^{22}\text{Na}$ reaction cross section. The effects of secondary particles from the target itself or from the experimental arrangement are believed to be small: The target stacks were only 100 mg/cm² thick and well collimated extracted beams were used in all cases. However, to account for the possibility of some low energy particles coming from beam-stopping devices, a 10% error was added in the case of ^{86}Rb and ^{88}Y production in ^{89}Y . These reactions are sensitive to (n,α) and $(n,2n)$ channels, respectively. The efficiency of the Ge(Li) detector was accurate to between 5% and 10%, depending on the peak energy. The reproducibility of the pho-

TABLE IV. Cross sections (in mb) for some radioactive isotopes produced in natural Zr as a function of the proton incident energy E_p (in GeV). "I" means independent cross sections. Others are cumulative.

E_p (GeV)	0.059	0.075	0.168	0.200	1.0	2.5	24.0
$^{74}\text{As}_I$					7.4 ± 1.5	4.8 ± 1.0	
^{75}Se			1.7 ± 0.8	3.9 ± 0.8	37 ± 7	22 ± 4	14.5 ± 2.9
^{83}Rb	2.9 ± 0.6	27 ± 5	37 ± 15	38 ± 8	34 ± 7	21 ± 4	16 ± 3
$^{84}\text{Rb}_I$		2.1 ± 0.4		4.5 ± 1.6	8.9 ± 1.8	6.0 ± 1.2	5.8 ± 1.2
$^{86}\text{Rb}_I$					5 ± 1	2.9 ± 0.6	
^{85}Sr		22 ± 7	28 ± 12	32 ± 8	30 ± 13	22 ± 8	18.8 ± 5.4
$^{88}\text{Y}_I$			52 ± 10	56 ± 11	27 ± 5.4	20 ± 4	
^{88}Zr	456 ± 91	232 ± 46	80 ± 16	79 ± 16	39 ± 8	28 ± 6	24.5 ± 5
^{95}Zr	10 ± 2	5.2 ± 1.0	2.3 ± 0.9	2.4 ± 0.6	2.8 ± 0.6	2.6 ± 0.5	2.8 ± 0.5
$^{92}\text{Nb}^m$					0.70 ± 0.14	1.20 ± 0.24	

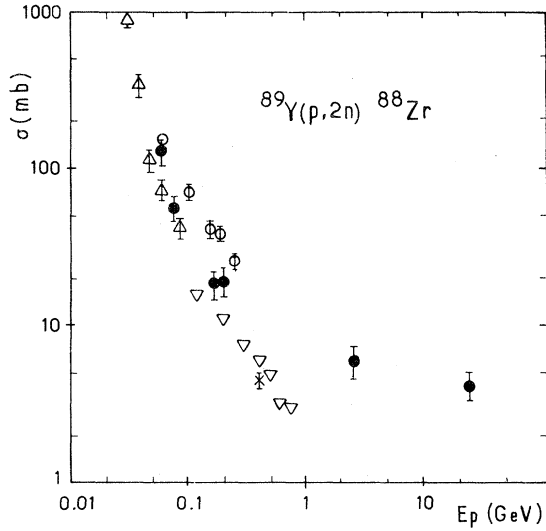


FIG. 1. Cross sections for the $^{89}\text{Y}(p,2n)^{88}\text{Zr}$ reaction versus energy. Symbols: ●, this work; △, Ref. 12; ○, Ref. 13; △, Ref. 14; and ×, Ref. 15.

topeaks integration and statistical errors varied with products between 3% and 10%. Weighted averages are reported in the case of multiple measurements. In most cases total uncertainties are around 20%, the largest errors being tied to resolution problems with the γ spectrometer, particularly for the 514 keV γ -ray emitter ^{85}Sr . Our results (filled symbols), together with those found in the literature (open symbols), are given for some excitation functions in Figs. 1–4.

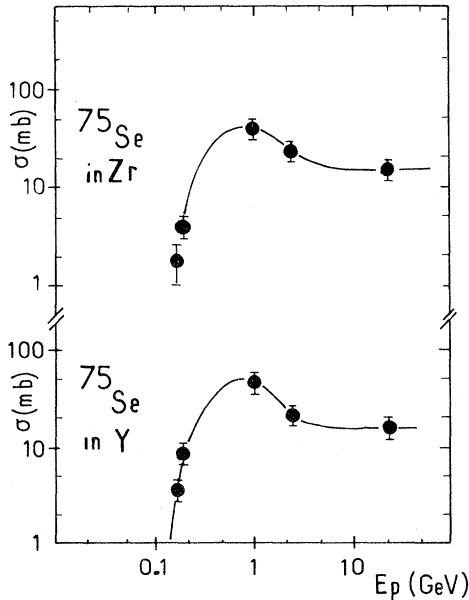


FIG. 2. Excitation functions for proton production of ^{75}Se in Zr and Y. Solid lines are our best manual fits.

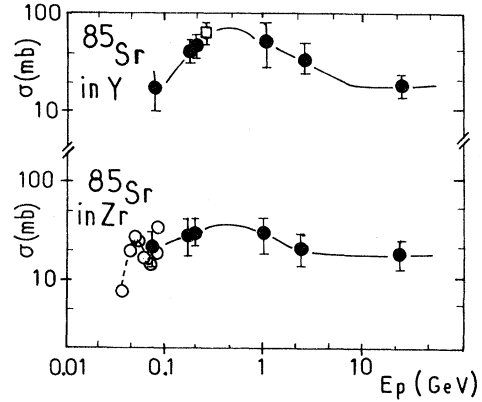


FIG. 3. Excitation functions for proton production of ^{85}Sr in Y and Zr. Symbols: ●, this work; □, Ref. 16; ○, Ref. 17. Solid lines as in Fig. 2.

(1) $^{89}\text{Y}(p,2n)^{88}\text{Zr}$ (Fig. 1). Our results agree within a factor of 2 with older measurements taken from Refs. 12–15.

(2) ^{75}Se produced in ^{89}Y and natural Zr (Fig. 2). Solid lines are our manual best fits. In both targets a maximum occurs in the 0.5–1.2 GeV energy region. The existence of such a maximum is clearly inferred from our cross section ratios at 1 and 24 GeV: 2.9 ± 0.8 in Y and 2.6 ± 0.7 in Zr (to be compared to the monitor cross section ratio of 1.5 at the same energies).

(3) ^{85}Sr produced in Y and natural Zr (Fig. 3). Our results are in good agreement with Refs. 16 and 17. A maximum is likely to occur between 0.4 and 0.8 GeV. The low energy peak in the case of the Zr target, inferred from the data of Ref. 17, results from the $^{90}\text{Zr}(p,3p\ 3n)^{85}\text{Sr}$ reaction channel.

(4) $^{83,84,86}\text{Rb}$ from ^{89}Y (Fig. 4). ^{84}Rb and ^{86}Rb are independently produced through $(p,3p\ 3n)$ and

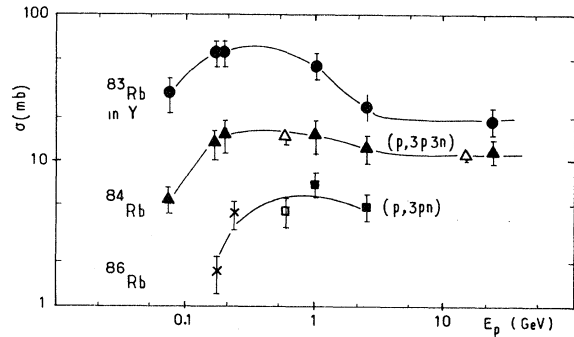


FIG. 4. Excitation functions for proton production of $^{83,84,86}\text{Rb}$ in Y. Filled symbols: this work; unfilled: Ref. 18; and crosses: Ref. 13. Solid lines as in Fig. 2. Reaction channels are quoted in the case of independent production.

TABLE V. Krypton cross sections (in mb) for Y target as a function of the incident energy E_p (in GeV).

E_p (GeV)	0.059	0.075	0.080	0.150	0.168	0.200	1.05	2.5	24.0
^{78}Kr	0.0024±0.0005	0.32 ±0.03	0.47 ± 0.16	9.1 ±1.0	14.8 ±1.5	24.4 ±2.4	29.2 ±2.9	13.7 ±1.3	10.9 ±2.6
^{80}Kr	2.25 ±0.23	3.0 ±0.3	2.1 ± 0.7	31.7 ±3.3	42.8 ±4.3	59.4 ±6.0	51.8 ±5.2	26.3 ±2.6	22.7 ±5.5
^{81}Kr	1.0 ±0.1	12.5 ±1.2	12.8 ± 4.1	44.7 ±4.6	55.8 ±5.6	74.0 ±7.5	53.0 ±5.3	27.3 ±2.7	24.0 ±5.8
^{82}Kr	3.9 ±0.4	65 ±6	47 ±15	63 ±6	72 ±7	89 ±9	57 ±6	30 ±3	28 ±7
^{83}Kr	71 ±9	50 ±5	32 ±10	88 ±9	74 ±7	88 ±9	63 ±6	34.7 ±3.5	32.4 ±7.8
^{84}Kr	7.3 ±1.0	8.1 ±0.8	6.1 ± 2.0	11.9 ±1.2	13.8 ±1.4	17.9 ±2.0	19.1 ±1.9	11.4 ±1.1	11.5 ±2.8
^{85}Kr		0.0039±0.0007	0.0071± 0.0023	0.035 ±0.004	0.060 ±0.006	0.095±0.010	0.350±0.035	0.22 ±0.08	0.234±0.064
^{86}Kr				0.0058±0.0021	0.0070±0.0047	0.014±0.009	0.105±0.017	0.044±0.010	0.061±0.017

($p,3pn$) reactions, respectively. Literature data are from Refs. 13 and 18.

B. Krypton isotopes

Cross sections for krypton isotopes are reported for Y and Zr targets in Tables V and VI. All results average two to four independent measurements weighted by individual errors. Our procedure for calculating the uncertainty was as follows: For each individual result, we quadratically added the errors on target preparation and impurities, measurement of ^{22}Na in monitoring, blanks, and hydrocarbons (the associated error was 50% of the correction), data reduction, mass discrimination, reextractions, and calibration. Many isotope ratios, available upon request, have a better than 1% precision. For all isotopes, cross sections are cumulative, except for the $^{89}\text{Y}(p,4p)^{86}\text{Kr}$ reaction. When necessary, they were corrected for incomplete decay of ^{83}Rb , using our values from Tables III and IV. All excitation functions for $^{78-86}\text{Kr}$ produced in Y and Zr targets are plotted in Figs. 5(a), (b), (c), and (d). Most of them show a maximum, probably in the vicinity of 0.5 GeV.

We also tried to measure krypton production in strontium. For this purpose, we prepared a vapor-deposited Sr target, 0.16 mg/cm² thick, which was irradiated at 168 MeV. Unfortunately, the deposit broke during preparation or handling of the stack, so that only the isotopic composition of spallation-produced krypton could be obtained. The result was as follows:

$$78/80/81/82/83/84/85$$

$$= 0.23 \pm 0.01 / 0.62 \pm 0.02 / 0.82 \pm 0.02 / 1 / 1.13$$

$$\pm 0.02 / 0.24 \pm 0.01 / 0.004 \pm 0.002$$

Together with the 730 MeV measurement of Ref. 19, this result provided a useful calibration for the Kr excitation functions in Sr, as estimated in the Discussion section.

C. Some general patterns

The existence of a maximum for excitation functions in the high energy region was already noted in the production of argon isotopes by spallation of Sc to Cu targets.⁶ In most targets, ΔA was larger than in the present study and the maxima occurred rather in the GeV region. Results from this laboratory,

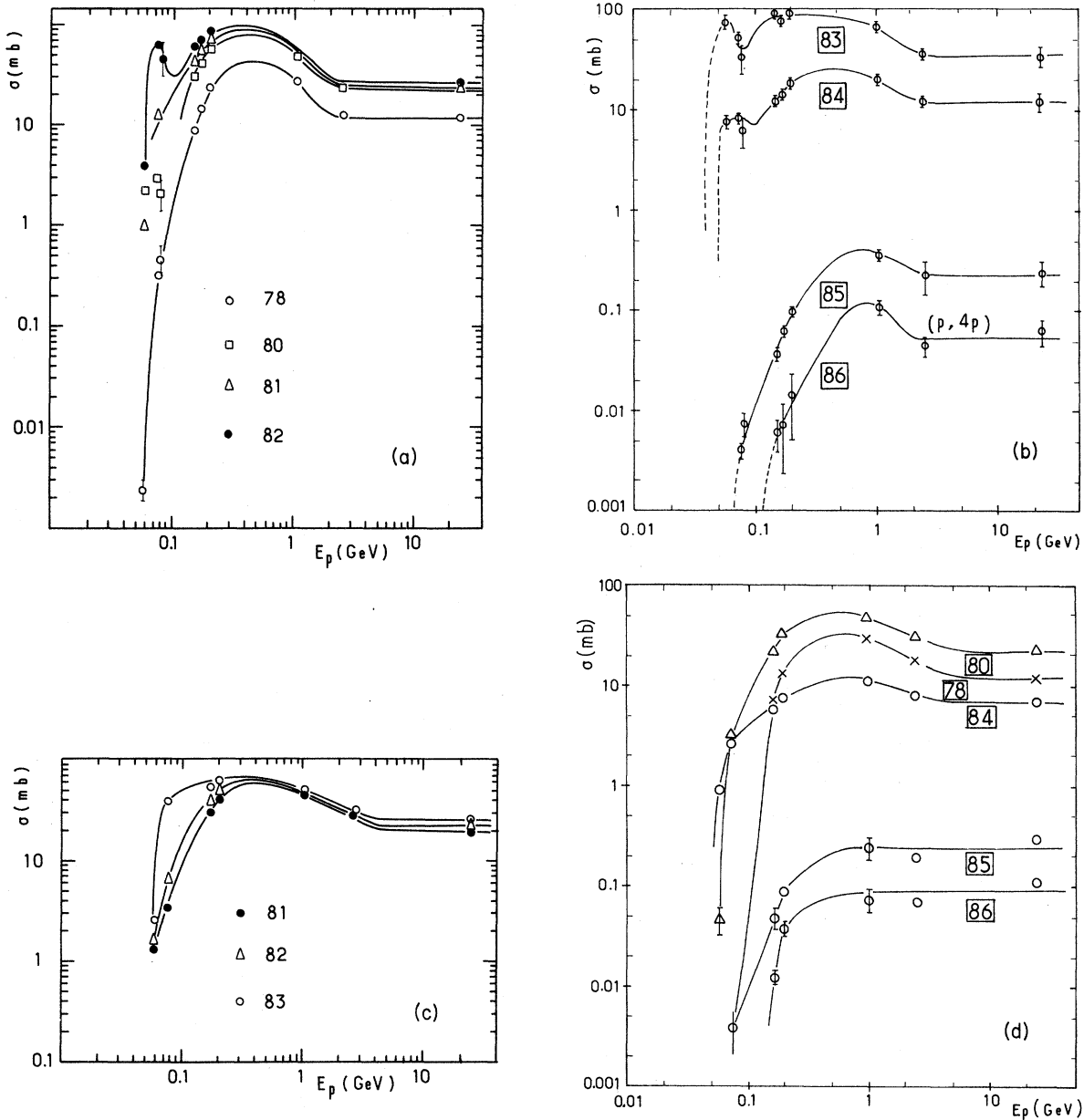


FIG. 5. Excitation functions for production of krypton isotopes in Y and Zr targets. All cross sections were measured in this work. Solid lines are mainly guides for the eye. Some experimental points were omitted to clarify the drawings. (a) $^{78,80,81,82}\text{Kr}$ production in ^{89}Y target; (b) $^{83,84,85,86}\text{Kr}$ in ^{89}Y ; (c) $^{81,81,83}\text{Kr}$ in Zr; and (d) $^{78,80,84,85,86}\text{Kr}$ in Zr.

yet to be published, also show that Kr isotopes produced in the spallation of Ag ($\Delta A=20-28$) have excitation functions with maxima at more than 1 GeV. Some ΔA dependence of the peak energy in the high energy spallation of medium mass targets may tentatively be inferred from available informa-

tion.

The cross section ratio between the estimated peak energy and the several GeV asymptote energy varies from 1.6 ± 0.4 to 4.3 ± 1.3 , without clear ΔA or target dependence.

TABLE VI. Krypton cross sections (in mb) for Zr target as a function of the incident energy E_p (in GeV).

E_p (GeV)	0.059	0.075	0.168	0.200	1.000	2.5	24.0
^{78}Kr		0.0028 ± 0.0005	7.11 ± 0.71	13.1 ± 1.3	28.3 ± 2.8	17.2 ± 1.7	11.6 ± 1.2
^{80}Kr	0.046 ± 0.014	3.14 ± 0.31	21.1 ± 2.1	31.6 ± 3.2	46.4 ± 4.6	28.9 ± 2.9	21.0 ± 2.1
^{81}Kr	1.33 ± 0.13	3.54 ± 0.21	30.8 ± 3.1	41.7 ± 4.2	46.7 ± 4.6	29.8 ± 3.0	21.8 ± 2.2
^{82}Kr	1.62 ± 0.16	6.6 ± 0.6	41.3 ± 4.1	52.6 ± 5.3	50 ± 5	32.1 ± 3.2	24.2 ± 2.4
^{83}Kr	2.55 ± 0.26	39.1 ± 3.9	54.8 ± 5.4	64 ± 6	52 ± 5	34.4 ± 3.4	26.9 ± 2.7
^{84}Kr	0.90 ± 0.09	2.64 ± 0.26	5.6 ± 0.6	7.45 ± 0.75	10.7 ± 1.1	7.6 ± 0.76	6.6 ± 0.7
^{85}Kr	< 0.001	0.0039 ± 0.0018	0.048 ± 0.011	0.088 ± 0.010	0.24 ± 0.06	0.19 ± 0.02	0.28 ± 0.03
^{86}Kr			0.0124 ± 0.016	0.038 ± 0.006	0.074 ± 0.019	0.070 ± 0.007	0.11 ± 0.01

D. Comparison with the Rudstam formula

We calculated our 119 measured cross sections for $^{78-86}\text{Kr}$ in Y and Zr, using the Rudstam-CDMD semiempirical formula¹⁰ and got the following patterns: (1) Excluding incident energies less than 100 MeV and low ΔA products (i.e., ^{85}Kr and ^{86}Kr) the average ratio F of calculated to experimental cross sections for the remaining 65 data is 1.2 ± 0.6 (1σ). This is quite a good result if one keeps in mind that the Rudstam formula was designed in 1966 at a time when experimental data were far less abundant than now. (2) The F ratio is about 2 at 24 GeV for the 78 to 83 krypton isotopes production in Y and Zr. (3) Over the 54 excluded data, 30 led to an F ratio ≥ 2.5 or ≤ 0.4 . Among them 14 gave a worse than 4 and seven gave a worse than 10 F ratio.

We also did the same calculation in the case of radioactive isotopes ($A=74$ to 88) that we measured in Y and Zr (77 cross sections). Excluding data for which $\Delta A \leq 5$ or $E_p < 100$ MeV, we got $F = 1.5 \pm 0.9$ (1σ) for the remaining 40 cross sections. The general patterns were similar to the case of krypton production.

IV. DISCUSSION

A main purpose of the present study was the prediction of the spallogenic component of krypton in samples of the lunar surface, as a function of their chemical composition and degree of shielding. Our experimental program led to the measurement of proton-produced krypton isotopes in Y and Zr targets. Little information was also obtained for Sr, and none for Rb and neutron-induced reactions. We thus developed new systematics, using our experimental values and all others available in this target range or its vicinity. As far as possible, we

tried to use simple observations involving the N/Z ratio of the target and the ΔA value between the target and product atomic masses. Also, it is well known that spallation reactions tend to favor neutron deficient products.

A. Estimation of unknown excitation functions

No formalism exists for the calculation of excitation functions for spallation reactions leading to various ΔA and involving a large range of incident proton or neutron energies, from a few MeV to several GeV. However, using the compound nu-

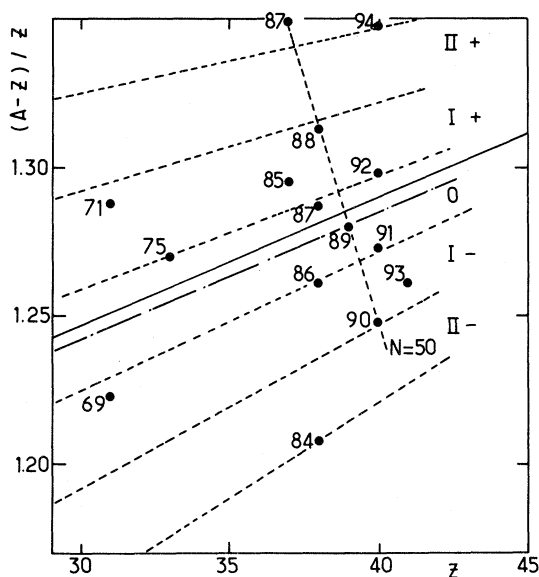


FIG. 6. Part of the $(A-Z)/Z$ versus Z plane. The solid line is the linear fit of Eq. (1), slightly translated to get it to pass through the ^{89}Y point (broken line). Dashed lines define several bands, $1/Z$ wide in the ordinate, where nuclei belong to the same arbitrary N/Z group. Points represent stable isotopes (denoted by their mass number A) for several elements.

TABLE VII. Compilation of proton induced reactions in Ga ($Z=31$) to Nb ($Z=41$) targets

Target	References
$^{69,71}\text{Ga}$	23, 24, 25, 26, 27
^{75}As	23, 25, 28, 29, 30, 31, 32
^{81}Br	33
^{88}Sr	34, 35
^{89}Y	12, 14, 16, 18, 37
^{90}Zr	17, 38, 39, 40
^{94}Zr	40
^{96}Zr	41, 42
^{93}Nb	43, 44

cleus²⁰ or the statistical model²¹ for lowest energies and the two-step model²² above 100 MeV should, in principle, make possible the calculation of most of the cross sections we need with a reasonable accuracy, but at the cost of many hours of use of the best modern computer. Considering only reaction channels leading to Kr isotopes in the four targets, Rb, Sr, Y, and Zr, we needed to calculate 300 to 400 excitation functions between the threshold and several GeV. Furthermore, to our knowledge, the statistical or hybrid-model calculations have not been applied to our target range and this would represent considerable work in order to get the precision we need (better than a factor of 2). Also, the two-step model does not always give good results.

Existing semiempirical fits^{10,36} do not cover the low energy region and have to be considered with caution in product and target-mass ranges where ex-

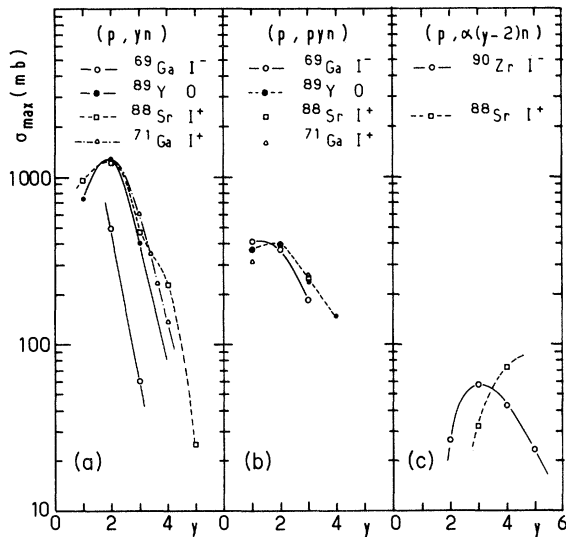


FIG. 7. Peak cross sections for some peripheral reactions in target nuclei belonging to various N/Z groups: (a) (p, yn) reactions; (b) (p, pyn) reactions; and (c) $(p, \alpha(y-2)n)$ reactions.

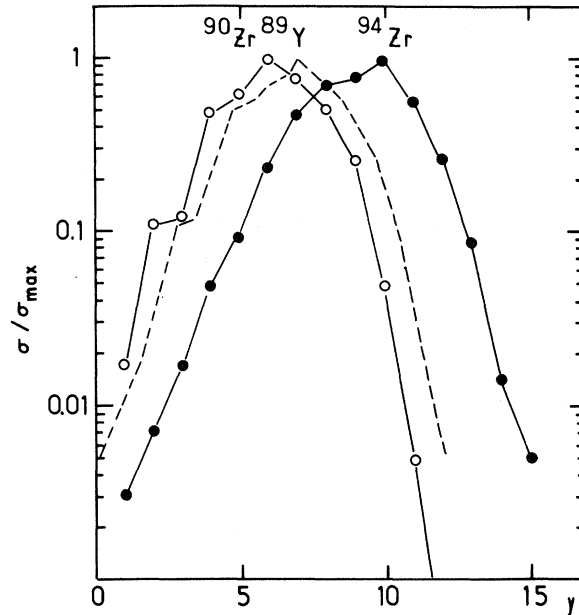


FIG. 8. $(p, 4pyn)$ reaction cross sections in ^{90}Zr and ^{94}Zr , normalized to their maximum values in both targets (solid lines), according to Belyaev *et al.* (Ref. 40). The quantity in the ordinate is thus $\sigma/\sigma_{\text{maximum}}$. The dashed line is interpolated (see text) for the same reaction channels in ^{89}Y .

perimental data are not very abundant.

As a point of departure, we will consider the position of an extended target nuclei range on the $(A-Z)/Z$ versus Z plane. For targets between Cu and Ag ($Z=29$ to 47), the best linear fit is given by

$$(A-Z)/Z = 0.00424 \times Z + 1.12. \quad (1)$$

In order to have a convenient reference line, we slightly translated the above linear fit to get it to pass through the ^{89}Y point. In Fig. 6, we represent part of the $(A-Z)/Z$ versus Z plane with the translated line of Eq. (1) and several bands ($1/Z$ wide on the ordinate) are denoted by a number and a sign. The "0" band comprises target nuclei that we define as similar to ^{89}Y by N/Z considerations. Other bands have a positive sign in the case of "neutron richer" targets and a negative sign otherwise. The number becomes larger with an increasing difference in ordinate.

We then plotted excitation functions $(p, xpyn)$ with $x=0-4$ and $y=0-12$ in Ga to Nb target elements or isotopes. A compilation of cross section sources, other than this work, is given in Table VII. Grouping by x values and band numbers leads to the following observations:

(1) If $E_p \leq 100$ MeV and $y > 2$, the peak section

tends to increase when the target nucleus becomes neutron richer. This effect is stronger for a given x value when y (i.e., ΔA) increases. It is illustrated in Figs. 7(a) and (b), where the peak cross section is plotted versus y for (p,yn) and (p,pyn) reactions in isotopic targets ^{69}Ga , ^{90}Zr , ^{89}Y , ^{88}Sr , and ^{71}Ga . More experimental data would clearly be useful to better establish the limits of the above effect. In Fig. 7(c) is plotted the peak cross section for $(p,\alpha(y-2)n)$ reactions. There, the main effect is the displacement of the most likely channel to higher y values when the target nucleus becomes neutron richer.

(2) It is reasonably safe to evaluate an unknown cross section by using the same reaction channel in a nucleus belonging to the same band, taking into account the above peak effect. When necessary, interpolation can be made between two y values.

(3) The same "band rule" and interpolation possibility apply for $E_p > 100$ MeV and reactions $(p,xpyn)$ for which $x \leq 2$. For $x > 2$ we made use of another observation, illustrated in Fig. 8.

(4) The cross section distribution versus y for a given x is simply translated along the y axis by a y value equal to the algebraic difference between the band numbers of two target nuclei. In Fig. 8 the maximum cross section for $(p,4pyn)$ reactions at $E_p = 1$ GeV in ^{90}Zr or ^{94}Zr is taken as unity. The dashed line is interpolated for ^{89}Y . In practice, a $(p,4pyn)$ channel in ^{87}Rb or ^{94}Zr (band III⁺) is equivalent to a $(p,4p(y-3)n)$ channel in ^{89}Y (band 0).

In the case of neutron incident particles, no systematics is possible, since few experimental cross sections exist under 20 MeV (Refs. 45–48) and none above. We made the first assumption that most excitation functions are the same for incident protons and neutrons after correction for threshold. This is likely to be true, at least if $E_n \geq 100$ MeV or $\Delta A \geq 5$. In some cases, adjustments could be made using available information for $(n,2n)$, (n,p) , and (n,α) channels. More questionable are the next assumptions concerning particular channels: $(n,2p)$ reactions were taken as 10% of the (n,p) reactions on the same target and $(n,p,2n)$ equivalent to $(p,2pn)$ reactions; (n,pn) and $(n,2pn)$ were taken as the average of the $(p,pn) + (p,2p)$ and the $(p,2pn) + (p,3p)$ reactions channels, respectively. Although this looks like a recipe, the calculation of the Kr isotopes distribution in lunar rocks agrees reasonably well with experiments, as we will see in the next section. Finally, estimating an unknown excitation function followed three steps:

(1) Identification of all possible reaction channels

in the case of cumulative cross sections or multiple-isotopes targets.

(2) For every channel, a search for an analog reaction in the same band and application of the above systematics, taking into account the peak displacement and threshold value, interpolating if necessary between two bands or two y numbers. If necessary, evaluation of the neutron channels.

(3) Building of all excitation functions and making of summations over target isotopes and radioactive decay chains. It must be emphasized that numerous reaction channels are responsible for the formation of krypton isotopes in Sr and Rb targets, so that some systematic bad trends are expected to compensate for each other in calculating cumulative cross sections. In the case of strontium, we got some normalization from our measurements at 168 MeV and those of Ref. 19 at 730 MeV. The most difficult cases were ^{84}Kr and ^{86}Kr , since neutron-induced reactions were the most important.

We tested our procedure by calculating cross sections for $^{78-84}\text{Kr}$ in Y and Zr targets and found agreement with our experimental values (within error bars) for all isotopes and all proton incident energies, except for some cases where the slope of the excitation function is very strong.

Our experimental results in Y were largely used in our systematics but not those in Zr, so that the observed agreement between calculated and measured values can be considered to be significant. It is illustrated in Table VIII where the ratio F of calculated (from our systematics) over measured cross sections in Zr targets is given versus the proton en-

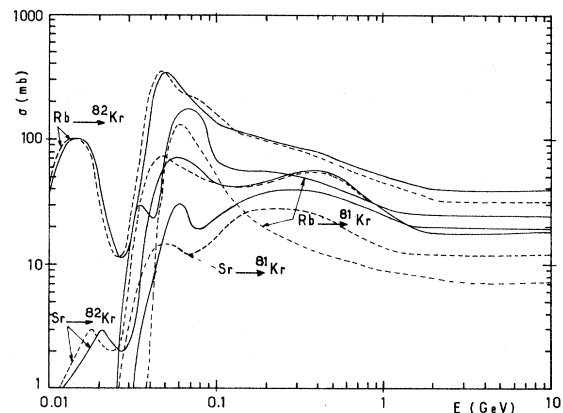


FIG. 9. Estimated excitation functions for proton-induced (continuous line) and neutron-induced (dashed line) reactions in Rb and Sr targets leading to ^{81}Kr and ^{82}Kr . "Bumps" at low energy correspond to specific reaction channels such as $^{85}\text{Rb}(n,\alpha)^{82}\text{Kr}$.

TABLE VIII. Ratio of calculated and experimental Kr isotopes cross sections in Zr versus the proton incident energy.

E_p (GeV)	0.075	0.200	1.0	24
^{78}Kr		0.80	0.69	0.70
^{80}Kr		1.03	0.87	0.87
^{81}Kr	1.44	0.73	1.05	1.13
^{82}Kr	1.29	0.79	1.03	0.85
^{83}Kr	0.45	0.65	1.15	0.90
^{84}Kr	0.57	0.97	1.34	1.78

ergy at 0.075, 0.2, 1.0, and 24 GeV. $^{85,86}\text{Rb}$ are produced in Zr through very particular reaction channels such as $(p,6p)$ and were not calculated. We also excluded the ^{78}Kr and ^{80}Kr production at 75 MeV since we had no information on reaction channels of interest for this energy. The remaining 22 data give an average ratio $F=0.96\pm 0.31$ (1σ).

The resulting estimated excitation functions will be used in the next section for calculating the production rates of krypton isotopes in the moon. A sample of the calculated (from systematics) excitation functions is given in Fig. 9 for production of ^{81}Kr and ^{82}Kr in Rb and Sr targets bombarded by protons and neutrons. Bumps in Fig. 9 come from the fact that we dealt with many reaction channels to get cumulative cross sections.

Compared to Y and Zr, Rb and Sr targets are expected to be much more effective for producing the neutron-rich $^{84-86}\text{Kr}$ isotopes and neutron-induced reactions are of prime importance.

Most of the cross sections we needed to calculate in Rb and Sr targets were outside the range of E_p and ΔA , where the Rudstam formula can be applied and no systematic comparison could be made. Also, this formula does not fit well the data of Ref. 19 for Kr production in Sr at $E_p=730$ MeV. However, we are looking for the possibility to reactualize the parameters of the Rudstam formula in the $A=80$ to $A=110$ target mass region, using all newly available experimental data.

B. Calculation of cosmogenic krypton

The moon or any other atmosphere-free object in the solar system can be considered a very thick target exposed to the bombardment of the primary flux of solar and galactic cosmic rays. Cascade-evaporation processes develop a large flux of secondary particles and nuclear reactions still occur at a depth of several meters. The production rate $P(d)$ of an isotope by a given nuclear reaction at a depth d can be calculated using the expression⁵:

$$P(d) = N \int_E \frac{dJ}{dE}(E, d) \sigma(E) dE, \quad (2)$$

where $\sigma(E)$ is the excitation function for this reaction, N is the number of target atoms per unit mass, and $(dJ/dE)(E, d)$ is the differential flux of interacting particles at that depth. The differential flux between 0 and 500 g/cm² at the lunar surface was calculated according to Ref. 5. Using our measured or estimated excitation functions, we calculated the production rate and isotopic composition of krypton in the same lunar rocks as in Refs. 3 and 4, assuming a surface erosion rate of 0.3 g/cm² per million years.

A detailed discussion of our procedures, together

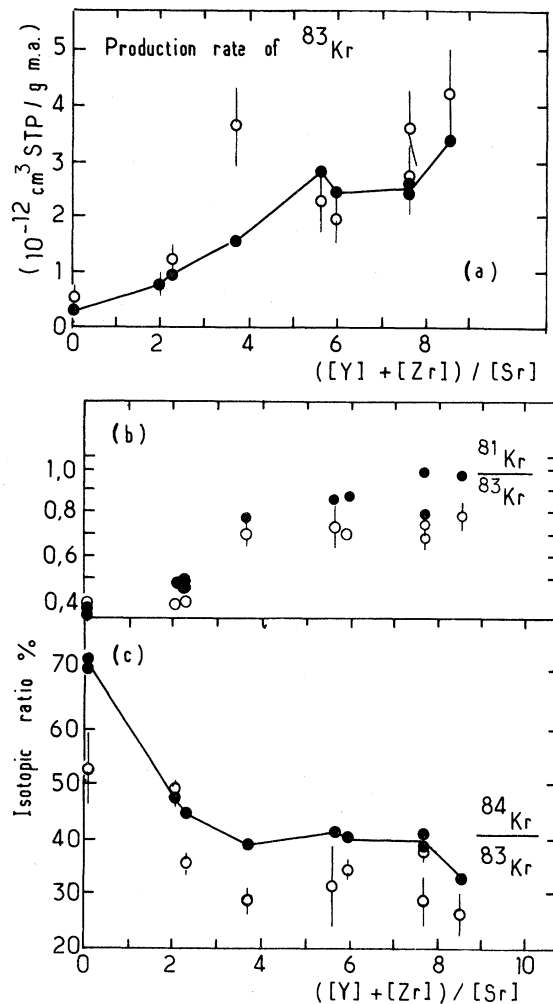


FIG. 10. Production rate of ^{83}Kr (a) and production ratios $^{81}\text{Kr}/^{83}\text{Kr}$ (b) and $^{84}\text{Kr}/^{83}\text{Kr}$ (c) versus the ratio of the main target element concentrations in lunar samples. Full circles and continuous lines are calculated values; open circles are experimental values (Ref. 3).

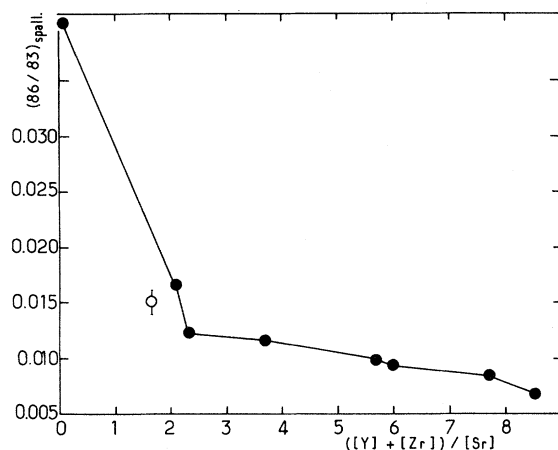


FIG. 11. Calculated $^{86}\text{Kr}/^{83}\text{Kr}$ cosmogenic ratio in lunar samples. Abcissa and symbols as in Fig. 10. The only experimental point is from Ref. 2.

with an analysis of our calculations, will be published elsewhere. In the framework of this paper, mostly devoted to nuclear processes, we merely want to give some cosmochemical implications of our new data:

(1) The production rate of ^{83}Kr (reference isotope) is predicted with a precision better than 33% (1σ). There exists a tendency to get less ^{83}Kr in strontium-rich samples. Figure 10(a) shows the calculated and measured production rates of ^{83}Kr versus the ratio $(Y + Zr)/\text{Sr}$ of the main target element concentrations in the nine selected lunar samples.

(2) The quotients of predicted to observed isotopic ratios of cosmogenic krypton averaged over nine

well-documented lunar samples are 1.09 ± 0.13 , 1.05 ± 0.08 , 1.19 ± 0.12 , 1.13 ± 0.04 , and 1.23 ± 0.16 , respectively, in the case of $^{78}\text{Kr}/^{83}\text{Kr}$, ^{80}Kr , ^{83}Kr , $^{81}\text{Kr}/^{83}\text{Kr}$, $^{82}\text{Kr}/^{83}\text{Kr}$, and $^{84}\text{Kr}/^{83}\text{Kr}$ ratios. $^{81}\text{Kr}/^{83}\text{Kr}$, $^{84}\text{Kr}/^{83}\text{Kr}$, and $^{86}\text{Kr}/^{83}\text{Kr}$ ratios appear to be somewhat chemistry dependent, i.e., they depend on the relative concentration of the main target elements, as visualized in Figs. 10(b), 10(c), and 11. In strontium rich samples, the first ratio is lower and the two others are higher than in yttrium- and zirconium-rich samples.

(3) The calculated cosmogenic ratio $^{86}\text{Kr}/^{83}\text{Kr}$ is chemistry dependent, as shown in Fig. 11. This ratio is of particular interest, since it is largely used for correcting the primordial component of krypton, trapped during condensation and solidification processes in the solar system. Until now, the adopted value 0.015 had been measured in a single Apollo-12 basalt, exceptionally rich in cosmogenic krypton.² A calculation of the $^{86}\text{Kr}/^{83}\text{Kr}$ cosmogenic ratio in that sample would not be realistic, since its high exposure age would imply a very large correction for erosion effects.

(4) The low energy (around 50 MeV) irradiation of strontium targets may imply an overestimation of exposure ages calculated by the Kr-Kr method.¹ This effect, limited to strontium-rich samples, increases with shielding between 5 g/cm² (10%) and 100 g/cm² (25%) and is expected to be somewhat compensated for by erosion. It is due to the shape of excitation functions of $^{80,81,82}\text{Kr}$ for the low energy irradiation of Sr and should be checked by more measurements.

TABLE IX. Cross sections of some radionuclides produced in the spallation of Y and Zr targets versus the proton energy E_p . E_γ is the energy and I_γ the branching intensity of the measured γ ray for each product isotope.

Isotope	E_γ (MeV)	I_γ (%)	Half-life in days (d) or years (y)	σ in Y (mb)			σ in Zr (mb)		
				$E_p = 1.005$	2.5	24 GeV	$E_p = 1.005$	2.5	24 GeV
^7Be	0.478	10.35	53.3 d	10.0 ± 2.0	12.0 ± 2.4		10.0 ± 4.5		
^{22}Na	1.275	99.93	2.602 y		1.6 ± 0.3	2.2 ± 0.4			1.6 ± 0.3
^{46}Sc	0.889	100	83.8 d		3.4 ± 0.4	3.5 ± 0.4		3.1 ± 0.4	3.1 ± 0.4
	1.120	100							
^{48}V	0.984	100	15.98 d	1.1 ± 0.2	3.5 ± 0.4		0.95 ± 0.15	3.3 ± 0.4	
^{51}Cr	0.320	10.2	27.70 d	6.0 ± 2.0	9.4 ± 3.5		3.8 ± 1.3	8.6 ± 2.8	
^{52}Mn	1.434	100	5.59 d	2.5 ± 0.8	2.2 ± 0.4				
^{54}Mn	0.835	100	312.20 d	11.5 ± 6.0	14 ± 7	6.2 ± 3.0	9.5 ± 5.0	14 ± 7	6 ± 3
^{59}Fe	1.099	56.5	44.56 d	4.3 ± 1.0	5.4 ± 1.2				
^{56}Co	0.847	99.95	78.76 d	1.9 ± 0.4	1.9 ± 0.4	1.7 ± 0.3	1.2 ± 0.2	2.3 ± 0.5	1.5 ± 0.2
^{58}Co	0.811	100	70.78 d	14.3 ± 3.6	14.2 ± 2.3	10.3 ± 2.0	10.3 ± 3.0	12.2 ± 1.5	10.7 ± 2.0
^{60}Co	1.173	100	5.272 y		2.7 ± 0.8				
^{65}Zn	1.116	50.75	244.0 d	22.4 ± 3.0	15 ± 4	11 ± 3	17.2 ± 2.5	16 ± 2	10 ± 1.5

TABLE X. Cross sections of argon isotopes produced in the spallation of Y and Zr targets versus the proton energy E_p .

Ar	σ in Y (mb)			σ in Zr (mb)		
	$E_p=1.05$	2.5	24 GeV	$E_p=1.005$	2.5	24 GeV
36			0.5±0.1			0.34±0.16
38	1.1 ±0.2	3.0±1.0	5.6±1.0	0.9±0.7	4.1 ±1.4	5.1 ±0.8
39	0.54±0.15	2.7±0.5	3.7±0.6	1.0±0.2	2.5±0.3	3.3 ±0.4
42					0.20±0.06	0.17±0.03

V. CONCLUSION

An extensive study of nuclear reactions in Rb, Sr, Y, and Zr targets led us to calculate the production rates of krypton isotopes in a thick object (the moon) submitted to a flux of high-energy incident particles (cosmic rays). Precise cross sections for $^{78-86}\text{Kr}$ isotopes were obtained in Y and Zr targets bombarded with protons of nine energies between 0.059 and 24 GeV. Cross sections for a number of radioactive isotopes in the same two targets were also measured. Most excitation functions pass through a maximum between 0.4 and 0.8 GeV and a ΔA dependence of the peak energy is tentatively inferred from these results and others from our laboratory. A general survey of existing data for Ga to Nb targets permitted the development of new systematics for calculating unknown Kr cross sections in Rb and Sr targets. Neutron-induced reactions were also estimated. Applying measurements and calculations to the prediction of the cosmogenic component of krypton on the moon was quite successful. Compared to measured values in some selected samples, production rates and production ratios are now predicted with good accuracy for all Kr isotopes. The cosmogenic ratios $^{86}\text{Kr}/^{83}\text{Kr}$ and $^{81}\text{Kr}/^{83}\text{Kr}$ should depend mainly on strontium concentrations and this will have further developments in calculating exposure ages of extraterrestrial materials.

ACKNOWLEDGMENTS

We thank the following accelerator teams: Louvain-la-Neuve, Orsay, Saturne II, and CERN for their cooperation during the numerous irradiations which were necessary to carry out this work. We are indebted to K. Marti and R. C. Reedy for helpful discussions, and A. Mackenzie Peers for improving the English text. Valuable technical assistance was provided by F. Brout and C. Chouard. The research was sponsored by the Centre National de la Recherche Scientifique.

APPENDIX: LIGHTER RADIOISOTOPES AND $^{36,38,39,42}\text{Ar}$ PRODUCED IN Y AND Zr TARGETS

In the course of nondestructive γ counting of Y and Zr targets, some radioisotopes of no direct interest for our purposes were also measured. Cross sections for ^7Be , ^{22}Na , ^{46}Sc , ^{48}V , ^{51}Cr , $^{52,54}\text{Mn}$, ^{59}Fe , $^{56,58,60}\text{Co}$, and ^{65}Zn produced in Y and Zr bombarded with 1.005, 2.5, and 24 GeV are given in Table IX, together with nuclear constants of all radioisotopes. Because of poor statistics, some error bars are rather large. Also cross sections of $^{36,38,39,42}\text{Ar}$ were measured by mass spectrometry at 1 GeV or more. Results are given in Table X.

¹K. Marti, Phys. Rev. Lett. **18**, 264 (1967).

²K. Marti and G. W. Lugmair, Geochim. Cosmochim. Acta Suppl. **2**, 1591 (1971).

³C. M. Hohenberg, K. Marti, F. A. Podosek, R. C. Reedy, and J. R. Shirck, Geochim. Cosmochim. Acta Suppl. **10**, 2311 (1978).

⁴S. Regnier, C. M. Hohenberg, K. Marti, and R. C. Reedy, Geochim. Cosmochim. Acta Suppl. **11**, 1565 (1979).

⁵R. C. Reedy and J. R. Arnold, J. Geophys. Res. **77**, 537 (1972).

⁶S. Regnier, Phys. Rev. C **20**, 1517 (1979).

⁷D. D. Bogard, J. C. Huneke, D. S. Burnett, and G. J. Wasserburg, Geochim. Cosmochim. Acta **35**, 1231 (1971).

⁸J. Tobaillem, C. H. de Lassus St Genies, and L. Leveque, Saclay Report No. CEA-N-1466 (1), 1971.

⁹J. C. Gouillaud and J. L. Pedroza, Electron. Appl. Ind.

- 257, 35 (1978).
- ¹⁰G. Rudstam, *Z. Naturforsch* **21a**, 1027 (1966).
- ¹¹*Table of Isotopes*, 7th ed., edited by C. M. Lederer and V. A. Shirley (Wiley, New York, 1978).
- ¹²G. B. Saha, N. T. Porile, and L. Yaffe, *Phys. Rev.* **144**, 962 (1966).
- ¹³A. A. Caretto and E. O. Wiig, *Phys. Rev.* **115**, 1238 (1959).
- ¹⁴I. Levenberg, V. Pokrovsky, L. Tarasova, Van Chen-Peng, and I. Yutlandov, *Nucl. Phys.* **81**, 81 (1966).
- ¹⁵L. B. Church and A. A. Caretto, *Phys. Rev.* **178**, 1732 (1969).
- ¹⁶A. A. Caretto and E. O. Wiig, *Phys. Rev.* **103**, 236 (1956).
- ¹⁷M. V. Kantelo and J. J. Hogan, *Phys. Rev. C* **14**, 64 (1976).
- ¹⁸M. Lagarde-Simonoff and G. N. Simonoff, *Phys. Rev. C* **20**, 1498 (1979).
- ¹⁹H. Funk, F. Podosek, and M. W. Rowe, *Earth Planet. Sci. Lett.* **3**, 193 (1967).
- ²⁰V. F. Weiskopf, *Phys. Rev.* **52**, 295 (1937).
- ²¹M. Blann, *Phys. Rev. Lett.* **27**, 1550 (1971).
- ²²R. Serber, *Phys. Rev.* **72**, 1008 (1947).
- ²³J. W. Meadows, *Phys. Rev.* **98**, 744 (1955).
- ²⁴N. T. Porile, *Phys. Rev.* **125**, 1379 (1962).
- ²⁵N. T. Porile and S. Tanaka, *Phys. Rev.* **130**, 1541 (1963).
- ²⁶L. P. Remsberg and J. M. Miller, *Phys. Rev.* **130**, 2069 (1963).
- ²⁷N. T. Porile, S. Tanaka, H. Amano, M. Furukawa, S. Iawata, and M. Yagi, *Nucl. Phys.* **43**, 500 (1963).
- ²⁸G. Rudstam, thesis, University of Uppsala, 1956.
- ²⁹G. Rudstam and E. Bruninx, *J. Inorg. Nucl. Chem.* **23**, 161 (1961).
- ³⁰D. Morrison and A. A. Caretto, *Phys. Rev.* **127**, 1731 (1962).
- ³¹S. Kaufman, *Phys. Rev.* **126**, 1189 (1962).
- ³²J. B. Cumming, New York Operations Office Report 6141, 1954.
- ³³J. W. Meadows, R. M. Diamond, and R. A. Sharp, *Phys. Rev.* **102**, 190 (1956).
- ³⁴G. Albouy, M. Gusakow, N. Poffe, H. Sergolle, and L. Valentin, *J. Phys.* **23**, 1002 (1962).
- ³⁵D. R. Sachdev, N. T. Porile, and L. Yaffe, *Can. J. Chem.* **45**, 1149 (1967).
- ³⁶R. Silberberg and C. H. Tsao, *Astrophys. J. Supp.* **220**, 25, 315 (1973).
- ³⁷S. Regnier, *Lunar and Planetary Science X* (Lunar and Planetary Institute, Houston, 1979), p. 1013.
- ³⁸E. Unseren and E. O. Wiig, *Phys. Rev.* **122**, 1875 (1961).
- ³⁹L. B. Church, *Nucl. Phys.* **A162**, 643 (1971).
- ⁴⁰B. N. Belyaev, V. D. Domkin, Y. G. Korobulin, and L. M. Krizhanski, *Yad. Fiz.* **24**, 1177 (1976) [*Sov. J. Nucl. Phys.* **6**, 618 (1976)].
- ⁴¹N. T. Porile and L. B. Church, *Phys. Rev.* **133**, B310 (1964).
- ⁴²P. P. Strohal and A. A. Caretto, *Phys. Rev.* **121**, 1815 (1961).
- ⁴³G. Albouy, J. P. Cohen, M. Gusakow, N. Poffe, H. Sergolle, and L. Valentin, *J. Phys.* **24**, 67 (1963).
- ⁴⁴R. G. Korteling and E. K. Hyde, *Phys. Rev.* **136**, B245 (1964).
- ⁴⁵R. J. Prestwood and B. P. Bayhurst, *Phys. Rev.* **121**, 5 (1961).
- ⁴⁶B. P. Bayhurst, J. S. Gilmore, R. J. Prestwood, J. B. Wilhelmy, N. Jarmie, B. H. Erkila, and R. A. Hardekopf, *Phys. Rev. C* **12**, 451 (1975).
- ⁴⁷T. B. Ryves and P. Kolkowski, *J. Phys.* **67**, 529 (1981).
- ⁴⁸*Neutron Cross Sections*, compiled by M. D. Goldberg, S. F. Mughabghab, S. N. Purohit, B. A. Magurno, and V. M. Mag, Brookhaven National Laboratory Report No. BNL-325 (National Technical Information Service, Virginia, 1966), 2nd ed., 2nd suppl.